

Supporting Information

Energy level alignment and defect passivation realized by dipole molecular bridge for efficient and stable perovskite solar cells

Yi Luo^a, Jiankai Zhang^{a*}, Runhao Chen^a, Zebin Guo^a, Wenyi Wu^a, Yufei Guo^a,
Shiqiong Wang^a, Xin Xu^{b*}, Chengwen Huang^{c*} and Hai Zhou^{a*}

^a*School of Integrated Circuits, Dongguan University of Technology, Dongguan 523808,
Guangdong, China*

^b*DGUT-CNAM Institute, Dongguan University of Technology, Dongguan 523808, Guangdong,
China*

^c*School of Optoelectronic Engineering, Guilin University of Electronic Technology, Guilin
541004, Guangxi, China*

*Corresponding author. E-mail address: jkzhang@dgut.edu.cn (J. Zhang), xuxin@dgut.edu.cn
(X. Xu), cwhuang@guet.edu.cn (C. Huang), hizhou@dgut.edu.cn (H. Zhou)

Experimental section

Materials

The etching indium tin oxide (ITO) glass sheets ($RS \approx 10 \Omega/\text{sq}$) were purchased from Wuhu Jinghui Electronics Technology Co., Ltd. Jiuhua South Road Branch Office. Methylammonium chloride (MACl, 99.5%), methylammonium iodide (MAI, 99.5%), lead iodide (PbI_2 , 99.99%), Spiro-OMeTAD (99.8%), Formamidinium iodide (FAI, 99.5%), and phenyl C61 butyric acid methyl ester (PCBM) were purchased from Xi'an Yuri Solar Solutions Co., Ltd. Dimethyl sulfoxide (DMSO, 99%) was purchased from Alfa Aesar. Chlorobenzene (CB, 99.9%), Anhydrous Ethanol (99.8%), anhydrous isopropanol (IPA, 99.5%), dimethylformamide (DMF, 99%) and 2-Amino-4,5-imidazoledicarbonitrile (AIDCN) were purchased from Hunan Danchen Biotech Co., Ltd.

Device Fabrication

The etched ITO substrates were cleaned with water, isopropanol, and Ethanol by ultrasonic treatment for 20 min, respectively. The cleaned ITO is subjected to surface ultraviolet (UV) treatment for 15 minutes under ambient conditions. Then, a tin dioxide dilute solution (SnO_2 : water = 1:4) was spin-coated onto it at 4000 rpm in an ultra-clean glove box environment to prepare the electron transport layer and then annealed at 150°C for 30 minutes. The devices with the prepared electron-transporting layer undergo ultraviolet surface treatment for another 15 minutes before being introduced into a nitrogen-purged glove box. Inside the glove box, two-step deposition prepares the perovskite film: first, dissolving PbI_2 in dimethylformamide (DMF) and dimethyl sulfoxide (DMSO), with solvent ratios of 1:4 respectively; secondly, preparing a separate spin-coating solution by dissolving FAI, MACl and MAI in isopropanol. The first step involves spinning at 4000 rpm for 30 seconds after the dissolution process, followed by heat treatment at 70°C for one minute. In the second step, under nitrogen atmosphere, a separate spin-coating solution is prepared by dissolving FAI, MACl and MAI in IPA (isopropanol) with specific ratios, then

adding this to the center of the substrate while maintaining 4000 rpm rotation speed for coating for 35 seconds. Finally, after cooling to room temperature, a 100°C hot plate is used inside the glove box to heat treat (anneal) the perovskite layer for 50 minutes. For the addition of 2-Amino-4,5-imidazoledicarbonitrile (AIDCN), it is dissolved in IPA at concentrations varying with experimental design requirements and then spin-coated onto the film surface at 5000 rpm for 30 seconds before annealing at 100°C for five minutes. Subsequently, Spiro-OMeTAD as a hole transport layer is directly coated onto the AIDCN layer by spinning at 5000 rpm for 30 seconds. the metal Silver (200 nm) electrode was thermally evaporated in vacuum chamber at pressure set at $< 4 \times 10^{-4}$ Pa through a shadow mask, respectively. For each device, the active area was 0.01 cm².

Characterization

The crystal structure of the films was characterized at room temperature using a multifunctional X-ray diffractometer (Bruker D8 Advance, Germany). The surface and cross-sectional morphology of the films were observed using a field-emission scanning electron microscope (Thermo Fisher Scientific Verios G4 UC, Czech Republic). The surface topography, roughness, and surface potential of the films were measured using the Kelvin Probe Force Microscopy mode of an atomic force microscope (NT-MDT Ntegra Prima, Russia). The elemental composition, chemical states, and energy level structure of the materials were analyzed using an integrated XPS/UPS system (Thermo Fisher Scientific ESCALAB XI, Czech Republic). XPS measurements were performed using a monochromatic Al K α X-ray source. UPS measurements were performed using an unfiltered He I (21.22 eV) gas discharge lamp. All XPS spectra were calibrated using the C 1s peak at a binding energy of 284.8 eV. Chemical bonding information of the materials was obtained in transmission mode using an FTIR spectrometer (PerkinElmer Frontier, USA). The sample for FTIR measurement was prepared by dissolving PbI₂ and AIDCN powder in isopropyl alcohol (IPA), followed by spin-coating and annealing at 50°C for 5 minutes. The optical absorption properties of the films were measured using a UV-Vis-NIR

spectrophotometer (Agilent Cary 5000, Malaysia). The steady-state and time-resolved photoluminescence spectra of the films were measured using a fluorescence spectrometer (Edinburgh Instruments FLS 1000, UK) with an excitation wavelength of 400 nm. The photovoltaic performance of the perovskite solar cells was measured under simulated AM 1.5G illumination (100 mW cm^{-2}) from a Newport Oriel Sol3A Class AAA solar simulator (450 W Xenon lamp) using a Keithley 2612B source meter. The light intensity was calibrated with a certified silicon reference cell. A metal mask was used to define the active area during measurement. The external quantum efficiency spectra of the devices were measured using a dedicated spectral response system (SRF50 system). The transient photocurrent (TPC) and transient photovoltage (TPV) decays of the devices were obtained using a transient photocurrent-photovoltage measurement system (SouthPort SP-TPVC). The electron mobility and defect density of the devices were evaluated using the space-charge-limited current method. Dark current characteristics were tested using a Keithley 2612B source meter.

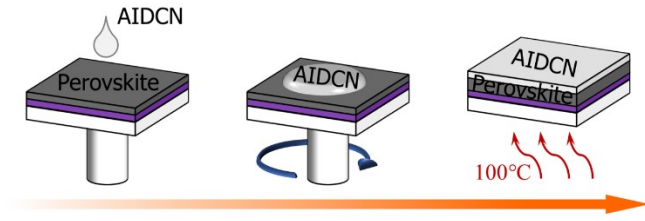


Figure S1. Schematic diagram of the preparation of the AIDCN passivation layer.

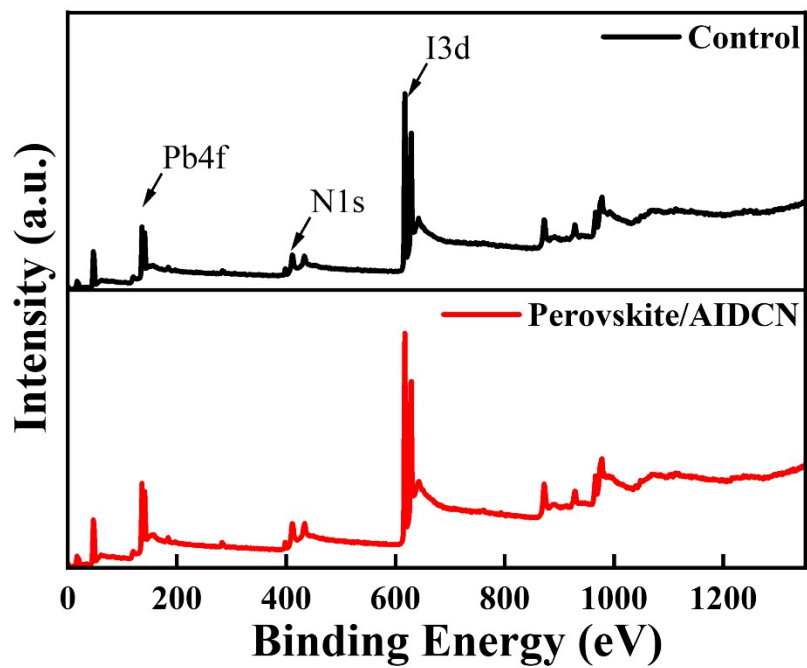


Figure S2. (a) Full XPS survey spectra of perovskite films with and without AIDCN modification.

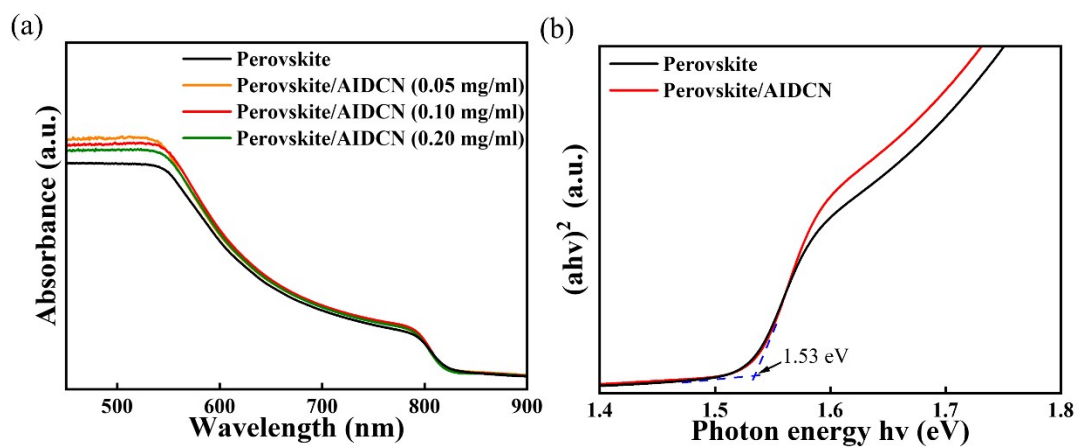


Figure S3. (a) UV-vis absorption spectra and (b) corresponding Tauc plots for the optical band gap determination of perovskite films with and without AIDCN modification.

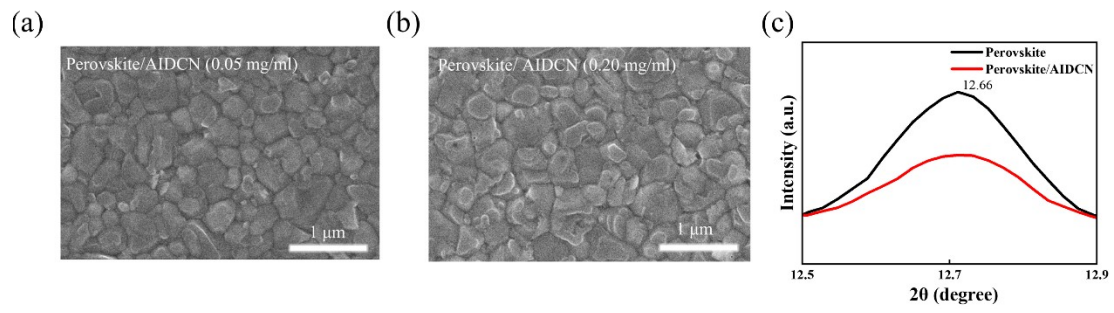


Figure S4. (a, b) Top-view SEM images and (c) magnified XRD patterns of perovskite films modified with varying concentrations of AIDCN.

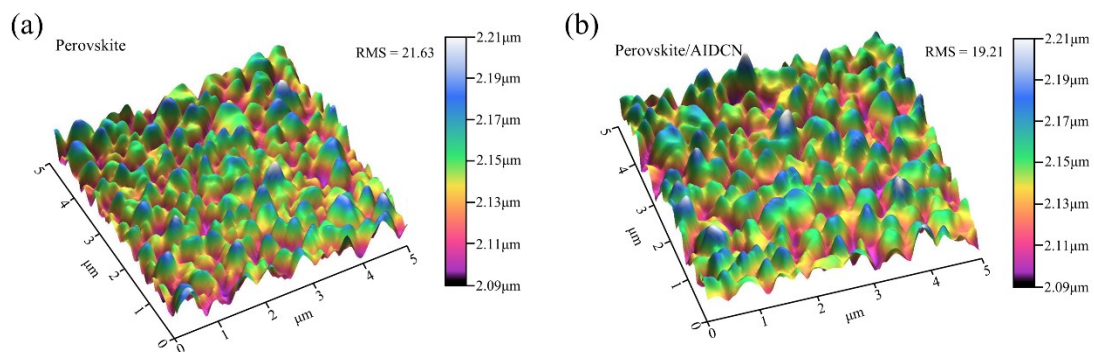


Figure S5. Three-dimensional surface morphology. (a, b) 3D AFM surface topography images of perovskite films with and without AIDCN modification.

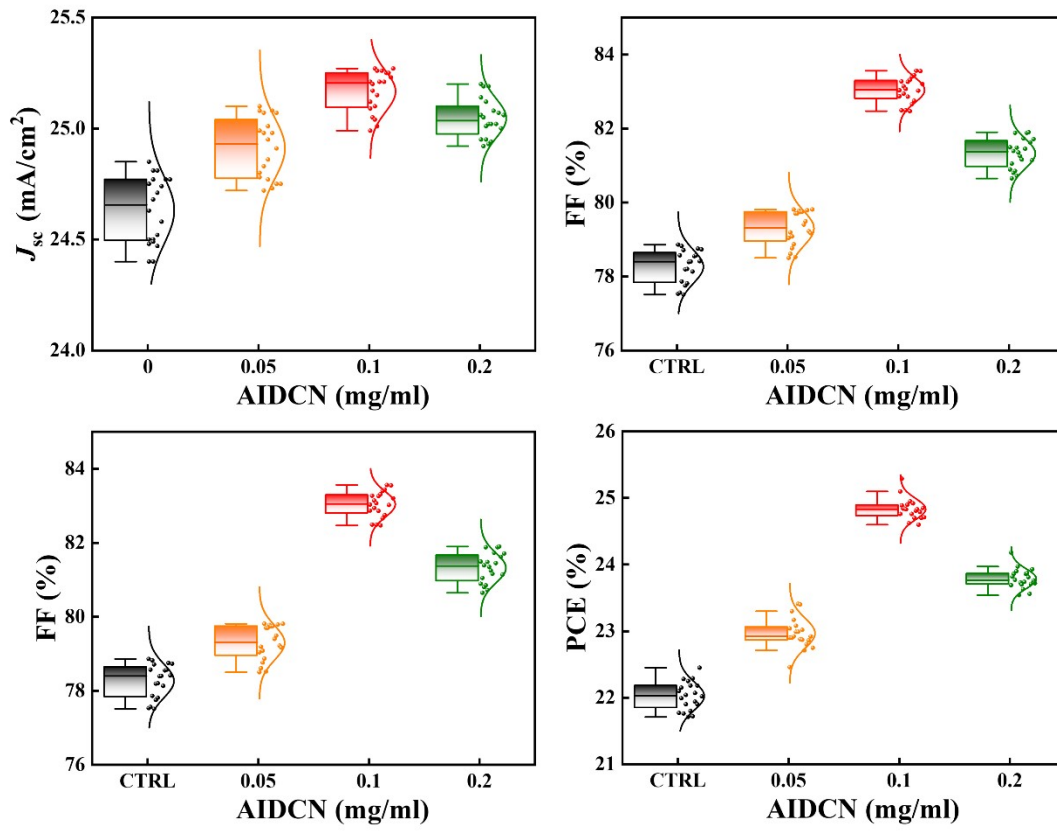


Figure S6. Statistical distribution of the power conversion efficiency (PCE) for control and AIDCN-incorporated devices.

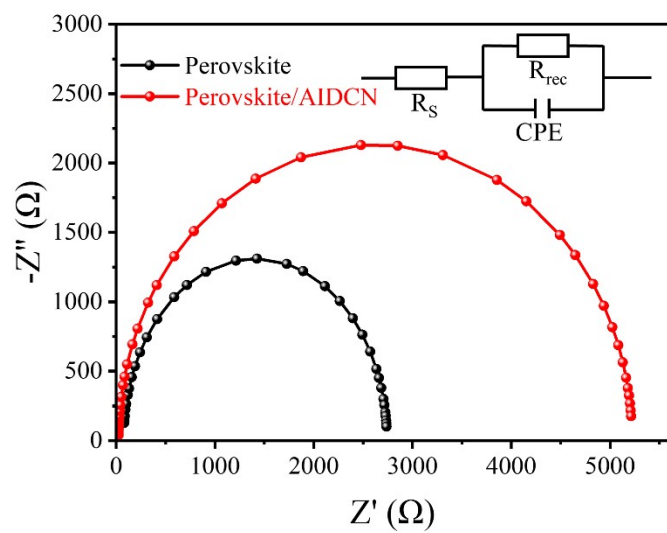


Figure S7. Nyquist plots of the control and AIDCN-modified PSCs.

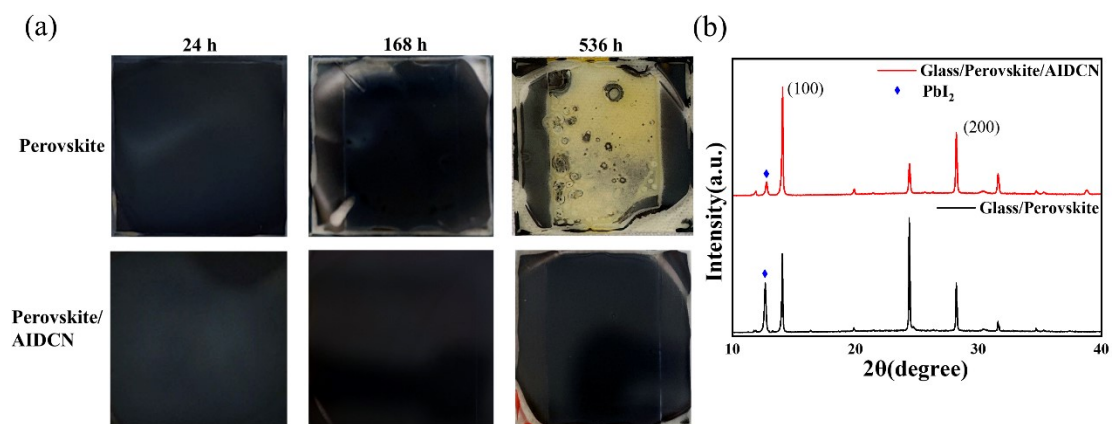


Figure S8. (a) Schematic layout of the control and AIDCN-incorporated device architectures. (b) XRD characterization of the control and AIDCN-modified perovskite films aged for 14 days.

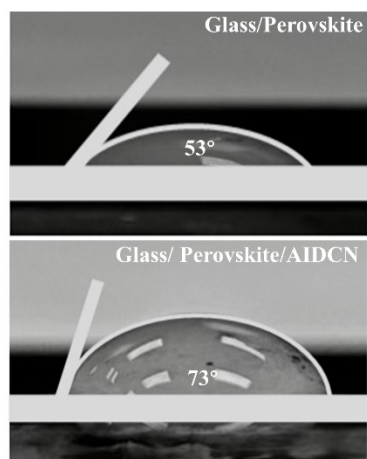


Figure S9. Contact angle measurements for evaluating the surface hydrophobicity of the control and AIDCN-modified perovskite films.

Table S1. The detail fitting parameters of the TRPL decay curves.

Sample	τ_1 (ns)	Fraction1	τ_2 (ns)	Fraction2	τ_{ave} (ns)
Control	11.81±0.717	14.40%	70.19±4.243	85.60%	60.47
Target	0.70±0.015	1.47%	46.95±2.016	98.53%	39.65

Table S2. The detail fitting parameters of the TRPL decay curves.

Sample	τ_1 (ns)	Fraction1	τ_2 (ns)	Fraction2	τ_{ave} (μ s)
Control	4.98 \pm 0.090	6.17%	75.70 \pm 0.699	93.83%	60.76
AIDCN	5.45 \pm 0.407	4.53%	114.79 \pm 1.957	95.47%	112.56

Table S3. The average photovoltaic parameters of PSCs modified without and with different concentrations of AIDCN. The average and deviation values are calculated from 20 devices from different batches.

Sample	V_{oc} (V)	J_{sc} (mA cm⁻²)	FF (%)	PCE (%)
Control	1.142	24.63	78.27	22.03
AIDCN 0.05 mg/ml	1.162	24.91	79.30	23.97
AIDCN 0.10 mg/ml	1.188	25.17	83.04	24.84
AIDCN 0.20 mg/ml	1.168	25.05	81.32	23.79